

Table S1. Donor Eyes used in this study. The dexamethasone induced expression of myocilin in these cells was characterized using PCR, western blots, and/or immunofluorescent microscopy as described (1). TM cells used in prior studies are indicated with the reference. NP=not published.

Donor	Age	Sex	cause of death	mean age	Reference
2016-1474	42	M	Anoxic brain damage		(2)
2017-0509	36	M	Pulmonary embolism		NP
2017-0611	38	F	Cardiac arrest		NP
2021-0755	21	F	Respiratory failure		(3)
2017-1472	41	M	Cardiac arrest		(2)
2018-1783	38	M	Respiratory failure		(3)
2019-0624	34	M	Hypoxemic cardiac arrest		NP
N27TM-6	27	F	Cardiomyopathy		(4)
N25TM-11	25	M	Unknown		NP
N35TM-11	35	M	Unknown		(4)
N17TM-2	17	M	Aortic aneurysm and renal failure		(5)
N27TM-2	27	F	Unknown		(4)
N27TM-8	27	F	Unknown		(6)
				31.4	
2021-1110	77	F	Lung cancer with metastasis		(2)
2021-1323	57	M	Cardiac arrest		(2)
2021-1328	75	M	Cardiac arrest		(2)
2021-1493	74	F	Subdural bleed		NP
2018-0070	54	M	Cardiac arrest		(3)
2018-1341	55	M	Myocardial infarction		(3)
2020-0984	69	M	Advanced Parkinson's and dementia		(3)
2022-0140	77	F	Cardiogenic shock		none
				67.2	

References

1. K. E. Keller *et al.*, Consensus recommendations for trabecular meshwork cell isolation, characterization and culture. *Exp Eye Res* **171**, 164-173 (2018).
2. Y. Y. Sun, Y. F. Yang, K. E. Keller, Myosin-X silencing in the trabecular meshwork suggests a role for tunneling nanotubes in outflow regulation. *Invest Ophthalmol Vis Sci* **60**, 843-851 (2019).
3. Y.-F. Yang, Y. Y. Sun, D. M. Peters, K. E. Keller, The effects of mechanical stretch on integrins and filopodial-associated proteins in normal and glaucomatous trabecular meshwork cells. *Front Cell Dev Biol* **10**, 886706 (2022).
4. M. S. Filla, J. A. Faralli, C. R. Dunn, H. Khan, D. M. Peters, NFATc1 regulation of dexamethasone-induced TGFB2 expression is cell cycle dependent in trabecular meshwork cell. *Cells* **12**, 504 (2023).
5. J. A. Faralli, R. W. Clark, M. S. Filla, D. M. Peters, NFATc1 activity regulates the expression of myocilin induced by dexamethasone. *Exp Eye Res* **130**, 9-16. (2015).

6. M. S. Filla, K. D. Dimeo, T. Tong, D. M. Peters, Disruption of fibronectin matrix affects type IV collagen, fibrillin and laminin deposition into extracellular matrix of human trabecular meshwork (HTM) cells. *Exp Eye Res* **165**, 7-19 (2017).

Table S2. Primers used for RT-qPCR. All sequences are given in the 5' to 3' direction.

Gene	Reverse Sequence	Forward Sequence
HPRT1	GGTCCTTTTCACCAGCAAGCT	TGACACTGGCAAAACAATGCA
SDHA	CACCACTGCATCAAATTCATG	TGGGAACAAGAGGGCATCTG
ITGB3 (β 3 integrin)	TTCTTCGAATCATCTGGCC	GTGACCTGAAGGAGAATCTGC
ITGA5 (α 5 integrin)	GTGGCCACCTGACGCTCT	TGCAGTGTGAGGCTGTGTACA
EDA+FN	GTCACCCTGTACCTGGAAACTTG	AGGACTGGCATTCACTGATGTG
EDB+FN	ACCTTCTCCTGCCGCAACTA	GGTGGACCCCGCTAAACTC
ACTA2 (α SMA)	GTGTTGCCCTGAAGAGCAT	GCTGGGACATTGAAAGTCTCA

Table S3 Primary Antibodies used for Flow Cytometry (FC) or Immunofluorescence (IF) Analyses

Antibody Name	Target	Application	Catalog Number and Supplier
Mouse IgG Isotype Control [15H6]	Neg. control	FC	GTX35014, GeneTex
Mouse monoclonal anti-integrin α v β 3 antibody, clone LM609	α v β 3	FC	MAB1976, Millipore Sigma
Mouse monoclonal anti-integrin α v β 3, clone [BV3]	α v β 3	IF	ab7166, Abcam
Mouse monoclonal integrin beta 1/CD29 antibody, clone 12G10	β 1	FC	NB100-63255, Novus Biologicals
Mouse monoclonal anti-integrin α 2 β 1 antibody, clone [16B4]	α 2 β 1	FC	ab24697, Abcam
Mouse monoclonal β -galactosidase, clone GAL-13	Neg. control	IF	G8021, Sigma-Millipore
Mouse monoclonal antibody, LIBS2, clone ab62	β 3	IF	MABT27, Millipore Sigma
Mouse monoclonal anti-integrin α 5 antibody, clone [P1D6]	α 5	FC	ab78614, Abcam
Mouse monoclonal integrin α 5, clone 10F6	α 5	IF	MA5-15568, Invitrogen
Mouse monoclonal anti-integrin α 4 antibody, clone HP2/1	α 4	FC	MAB1383, Millipore Sigma
Mouse monoclonal anti-integrin α 9+ β 1 antibody, clone [Y9A2]	α 9	FC	ab27947, Abcam
Rabbit polyclonal α -smooth muscle actin	α SMA	IF	ab5694, Abcam

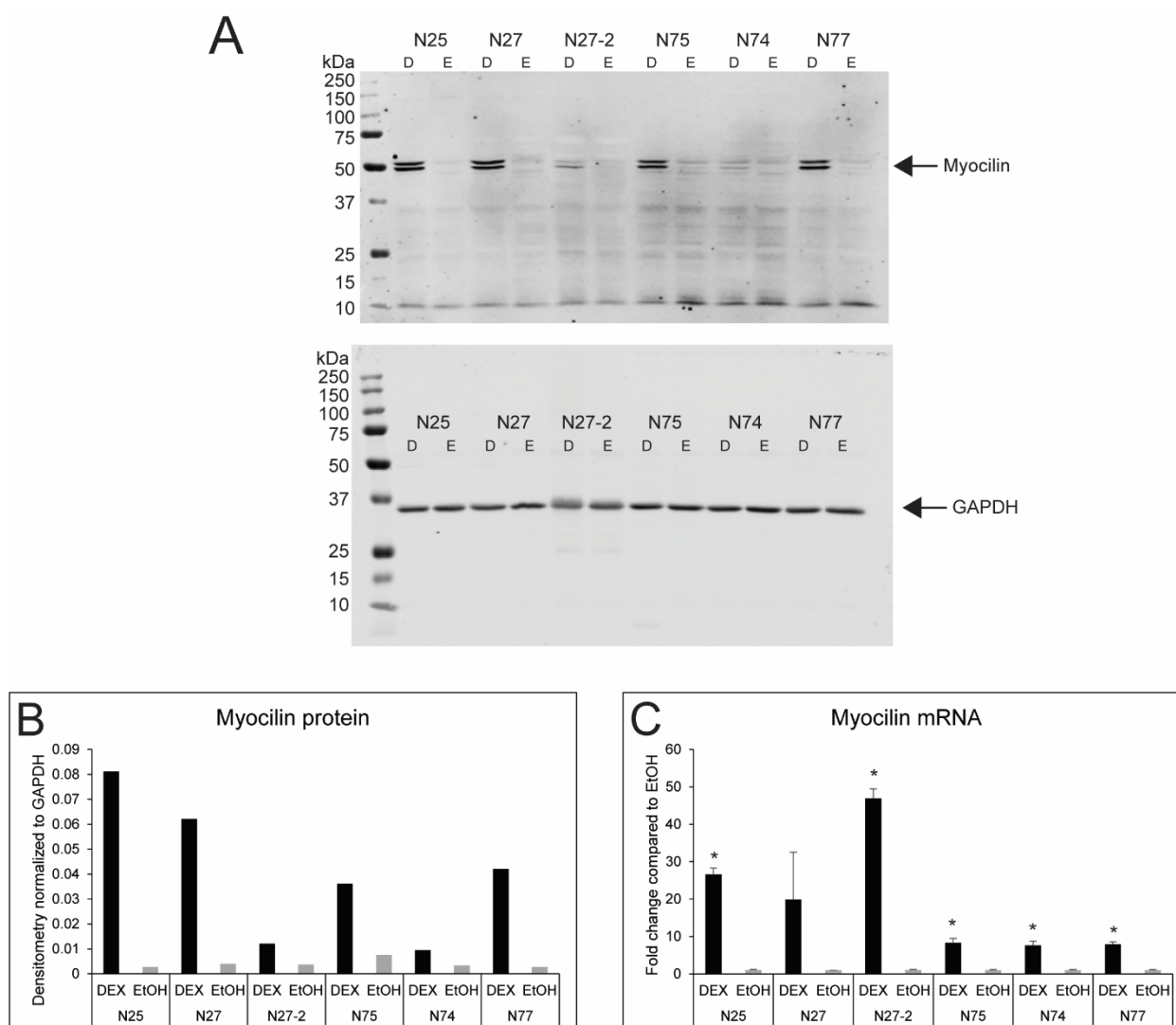


Figure S1 Characterization of myocilin expression in the 3 old TM cell (N74, N75, N77) and three young cell (N27-2, N27, N25) strains. TM cells as shown in Table 1 were grown in culture until confluent. One-week later cells were treated with dexamethasone (DEX; 500uM) or ethanol (EtOH) control for 7 days prior to harvesting lysates or RNA for western blot or RT-PCR analysis. (A) Western blots for myocilin (top; Millipore MBN866; 1:1000 dilution) or the loading control GAPDH (bottom; Abcam AB9485; 1:2500 dilution) showing DEX upregulated myocilin expression in all 6 cell strains. (B) Densitometry analysis of myocilin blot shown in (A) normalized to GAPDH. (C) RT-PCR results using primers specific for myocilin and SDHA (housekeeping gene). Data was analyzed by the DDCT method. n=3 technical replicates. DEX significantly different from EtOH by t-test, *p<0.05.

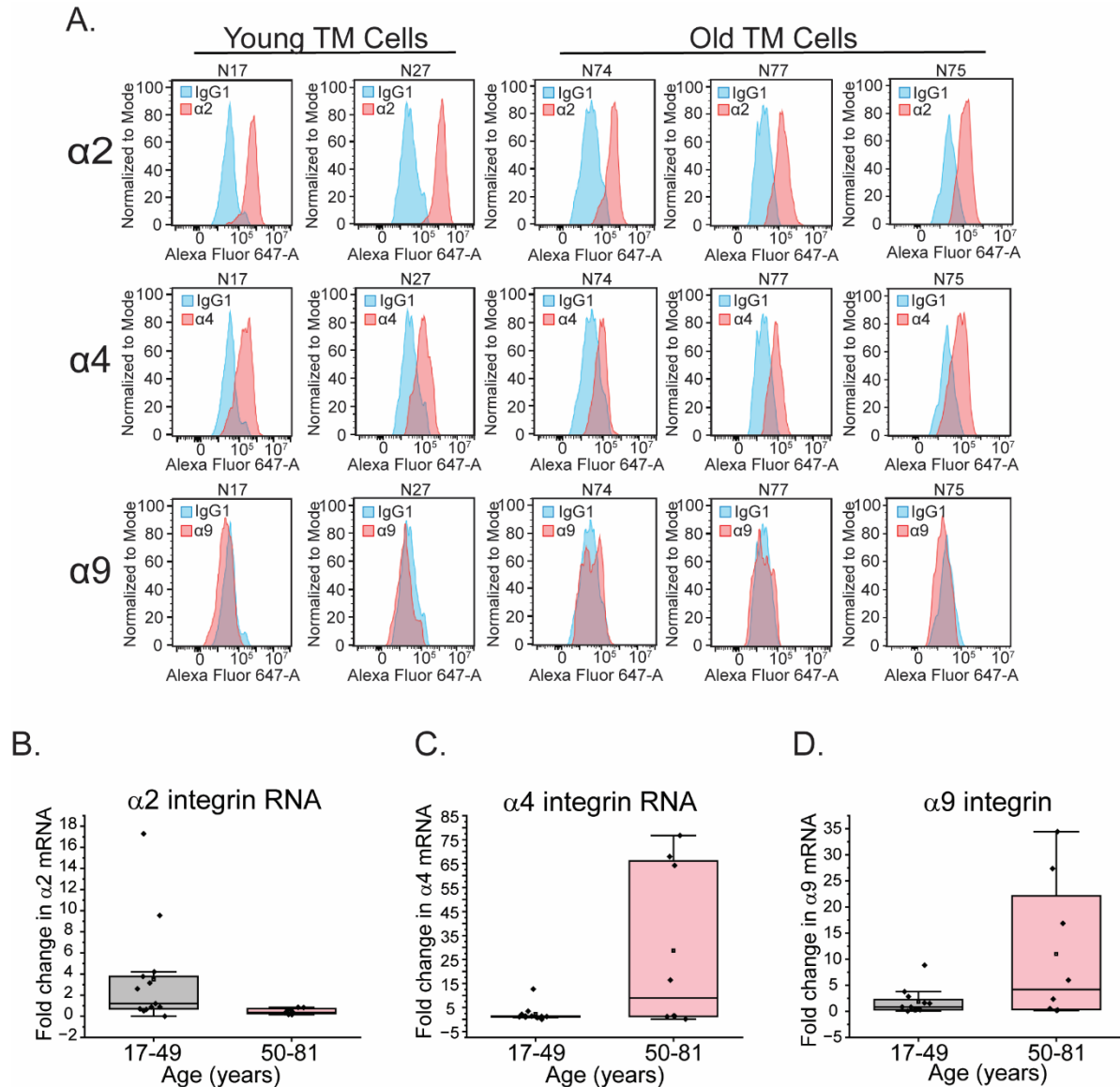


Figure S2 Levels of $\alpha 2$, $\alpha 4$, and $\alpha 9$ integrin subunits in young and old TM cells. (A) Flow cytometry showing levels of $\alpha 2$, $\alpha 4$, and $\alpha 9$ integrin subunits on two young cell strains (N17, N27) and three old cell strains (N74, N75 and N77). Blue peaks are cells labeled with control IgG, while pink peaks are cells labeled with either P1D6 mAb ($\alpha 5$ integrin; top panels), LM609 mAb ($\beta 3$ integrin subunit; middle panels), or 12G10 ($\beta 1$ integrin; bottom panels). Both young and old TM cells express similar levels of these integrin subunits (middle and bottom panels, respectively). (B) RT-qPCR analysis of $\alpha 2$, $\alpha 4$, and $\alpha 9$ integrin subunits. mRNA levels for $\alpha 4$ integrin subunit are statistically higher in TM cells from old donor eyes (pink) compared to levels found in TM cells from young donor eyes (gray). Changes are statistically significant (* $p < 0.05$). N=13 biological replicates/young, N=8/old.

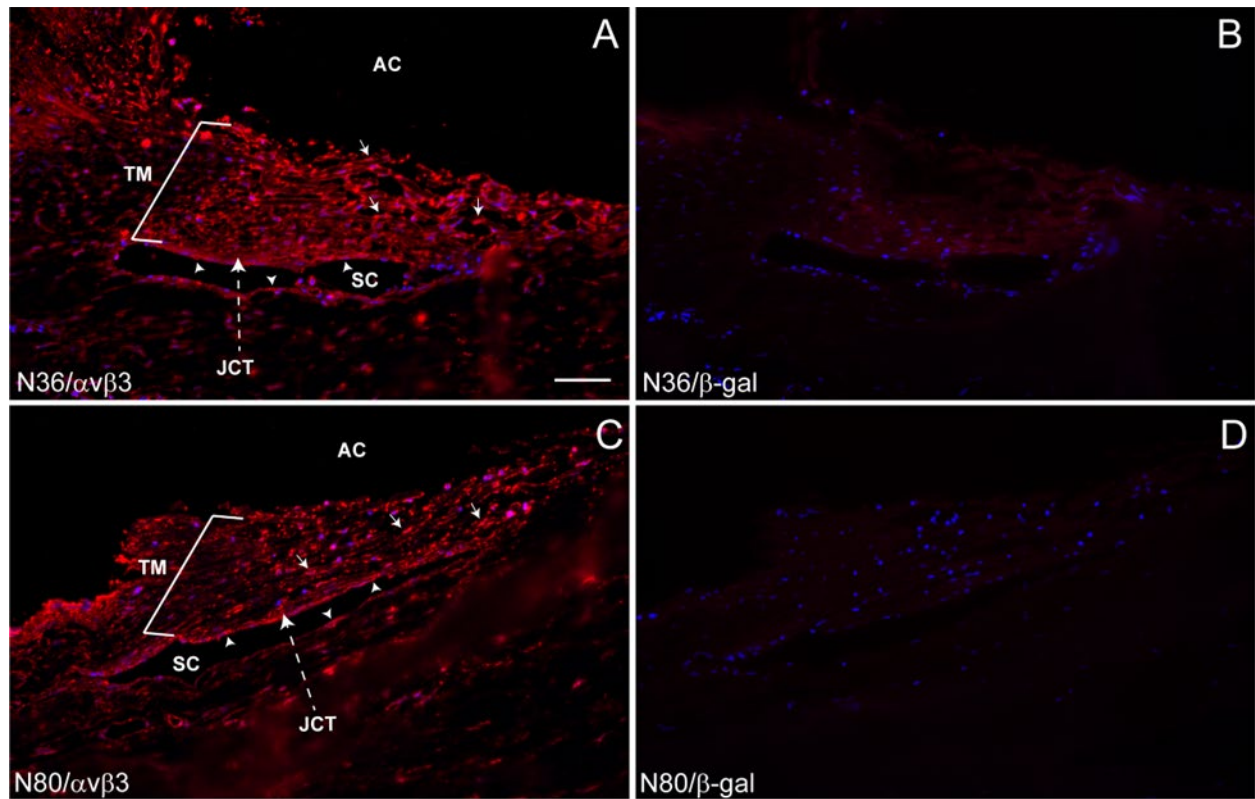


Figure S3. Immunolabeling for $\alpha v \beta 3$ integrin in anterior segments from young and old eyes. Sections of anterior segments from 36 (A & B) and 80 (C & D) year-old donor eyes were labeled overnight at 4°C with the monoclonal antibody [BV3] against $\alpha v \beta 3$ integrin (A & C) or the negative control monoclonal antibody GAL-13 against β -galactosidase (B & D). Bound primary antibodies were detected using Alexa 546-conjugated goat anti-mouse IgG. Nuclei were labeled with Hoechst 33342. Within the TM of both sets of tissue, positive labeling for $\alpha v \beta 3$ integrin was ubiquitous within the TM beam cells and JCT. Positive labeling was also present in both the inner and outer walls of the SC. In both young and old tissue samples, the $\alpha v \beta 3$ integrin labeling is clearly above the background labeling seen in the sections labeled with the negative control antibody. Arrows = TM beam cell labeling; arrowheads = SC endothelium labeling. AC = anterior chamber; TM = trabecular meshwork; JCT = juxtacanalicular tissue. Scale bar (A) = 50 μ m.

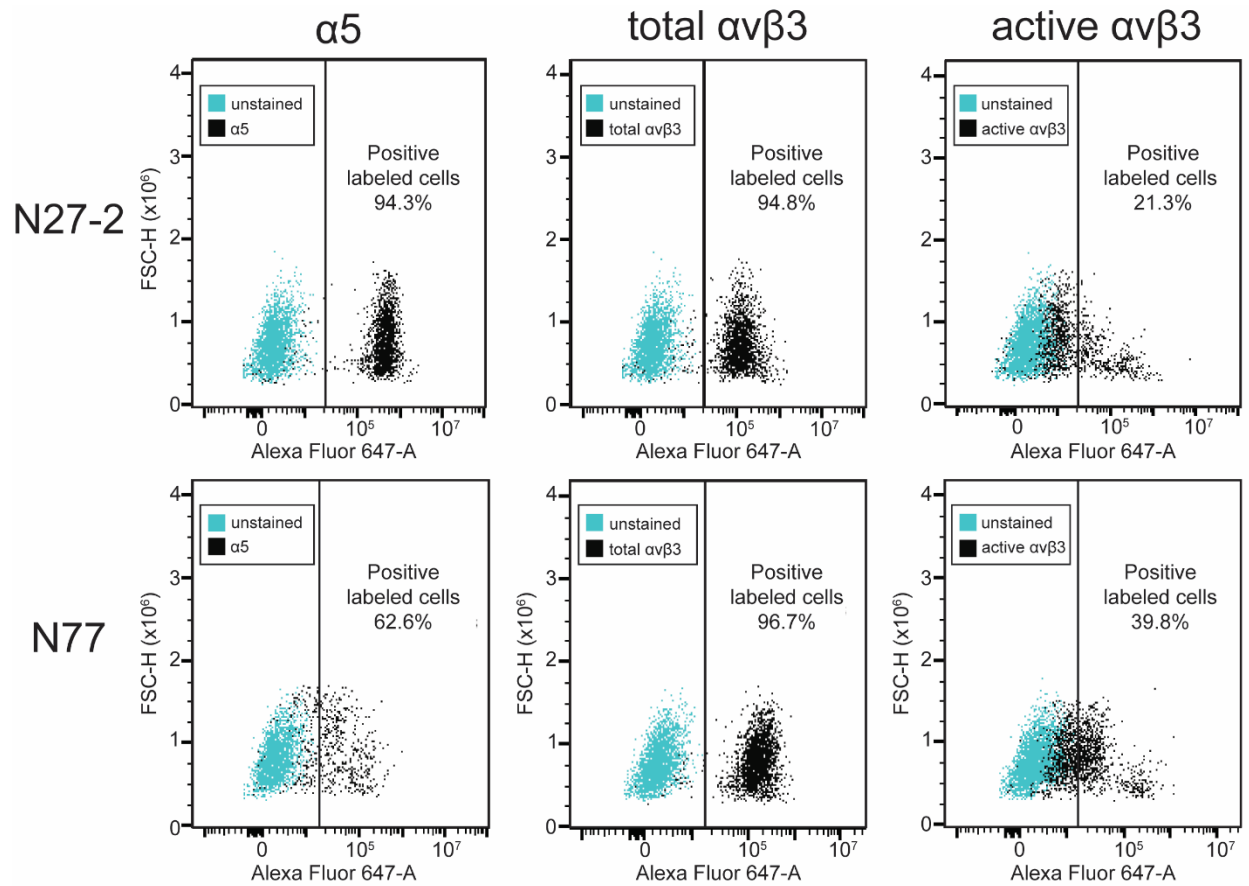


Figure S4 Dot plots of the percentage of N27-2 and N77 expressing $\alpha 5\beta 1$, $\alpha v\beta 3$ or activated $\alpha v\beta 3$ integrins. Cells were labeled with primary antibodies to integrins $\alpha 5$ (clone 10F6), $\alpha v\beta 3$ (clone [BV3]), or activated $\alpha v\beta 3$ (LIBS2) integrins as described in materials and methods. Plots show that an equal number of N27-2 and N77 express $\alpha v\beta 3$ integrin. However, a greater number of N27-2 cells express higher levels of $\alpha 5\beta 1$ integrins compared to the N77 cells. In contrast, a greater number of N77 cells express activated $\alpha v\beta 3$ integrins on their cell surface compared to the N27-2 cells. The solid vertical line indicates where the unstained population of cells.